Ultra Low Phase Noise DDS

fred harris
San Diego State University
fred.harris@sdsu.edu

Chris Dick
Xilinx Corp.
chris.dick@xilinc.com

Richard Jekel
Cubic Corp.
richard.jekel@cubic.com

ABSTRACT

Direct Digital Synthesizers traditionally use a phase accumulator and a phase-to-amplitude conversion mechanism to form complex samples of arbitrary frequency sinusoids. The CORDIC [1] algorithm is the most common phase-to-amplitude conversion processes. To obtain low levels of phase noise with a small number of iterations the DDS often employs a two pass algorithm in which the complex samples formed from high order phase bits are corrected by post processing with terms derived from low order phase bits. This paper presents a modified version of the CORDIC based DDS that suppresses the amplitude noise generated by the second pass phase correction. We then show that the amplitude noise suppression is equivalent to an embedded AGC. We then recast the second order normal recursive filter as a recursive version of the CORDIC and insert the equivalent AGC to stabilize the loop against finite arithmetic and signal growth due to the CORDIC. We show this to be a very interesting variation of the DDS.

1. INTRODUCTION

Many DSP algorithms in communication systems require values of a complex sinusoid (sine and cosine) of specific angles to accomplish a particular processing task. Examples include the DFT (discrete Fourier transform), the FFT (fast Fourier transform), digital up converters, digital down converters, and carrier recover loops [2]. Algorithms implemented in a high level language by a main frame or personal computer may compute the required sines and cosines from series expansions via a subroutine call as they are needed. Algorithms embedded in an ASIC (Application Specific Integrated Circuit) or in a fixed point microprocessor or FPGA can not afford the luxury of a subroutine call to a series expansion. They require another method to obtain values of the complex exponential for the specified value of argument.

In some algorithms, such as in the FFT, the values of the sines and cosines are known before hand and may be pre-computed and stored in a trig table. In other algorithms, the range of arguments may be too numerous to use a pre-computed table. We can still use the pre-computed table if we are willing to allow an acceptable approximation to the specified angle of the sine and cosine.

Let us examine the system effects of using approximations to the desired angles. The DDS (Direct Digital Synthesizer) is the standard mechanism to form a complex time series representing sample values of a sine and cosine. Figure 1 is the block diagram of a simple DDS formed by a 48-bit phase accumulator, a quantizer that extracts the 10 most significant bits from the accumulator, and a look up table addressed by the quantized 10-bit field to perform the phase to complex sinusoid conversion.

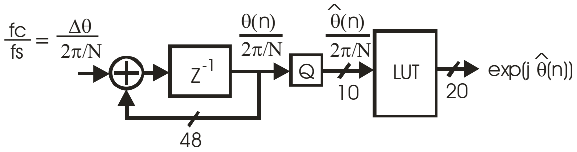
$\frac{fc}{fs} = \frac{\Delta\theta}{2\pi/N}$
Z^{-1}
$\frac{\theta(n)}{2\pi/N}$
$\frac{\hat{\theta}(n)}{2\pi/N}$
Q
10
LUT
20
$\exp(j\,\hat{\theta}(n))$
48

Figure 1. DDS: Phase Accumulator, Quantizer, and LUT

It is easy to verify [3] that the sequence of phase angle errors formed by the b-bit quantized address is a periodic sawtooth with amplitude proportional to the LSB, 2^{-b}. It is similarly easy to verify that the spectrum of the sinusoid formed with a sawtooth phase error contains a set of spurious spectral lines with the largest line 2^{-b} below the carrier spectral line. The largest spurious line is 6b dB below the carrier, where b is the quantized address width accessing the look up table. The signal formed with the 10-bit address shown in figure 1 should exhibit a spur 60 dB below the carrier. Figure 2, subplot(2,1,1) shows the -60 dB spur levels of a sinusoid formed with a 10-bit address while subplot(2,1,2) shows the reduction in spur level due to random dithering of the accumulator output prior to quantization.

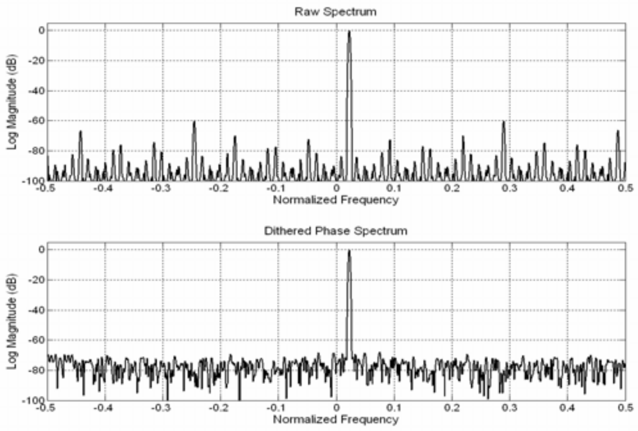

Figure 2. Spectra of 10-bit Angle DDS Output without and with Random Dither

To obtain spur levels 100 dB below the carrier we would require a 17-bit address for a table containing 131072 entries. The symmetry of sines and cosines allow some memory savings by storing the sinusoid samples in the first quadrant. Nevertheless, we are thus faced with the problem of doubling the table size for every 6-dB decrease in spurious level.

We can avoid the need for large tables by using the CORDIC algorithm to implement a set of elementary rotations requiring only shift and add operations and a look up table containing only b entries. Here we exchange a processing task for memory. The spur level of the time series formed by the CORDIC still has spurs 6b dB below the carrier but now b represents the number of rotation cycles implemented in the CORDIC. Figure 3 shows a modified DDS structure in which the length 2^b LUT is replaced by the CORDIC algorithm supported by a length b LUT. We delay detailed discussion of the CORDIC till a later section of this paper.

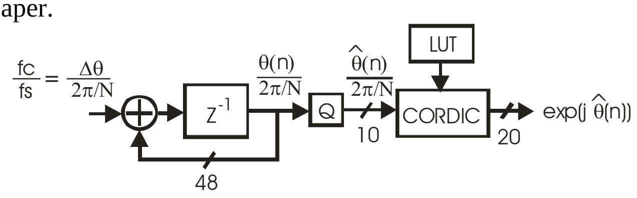

$\frac{fc}{fs} = \frac{\Delta\theta}{2\pi/N}$
Z^-1
48
$\frac{\theta(n)}{2\pi/N}$
Q
$\frac{\hat{\theta}(n)}{2\pi/N}$
10
LUT
CORDIC
20
exp(j $\hat{\theta}$(n))

Figure 3. DDS: Phase Accumulator, Quantizer, and CORDIC

2. SPURIOUS LEVEL SUPPRESSION

The quantization of the 48 bit accumulator to obtain the 8-bit address introduces a phase error term in the angle presented to the angle to amplitude conversion whether the conversion is performed by the look-up table or the CORDIC algorithm. The effect of the angle approximation is seen in (1): the angle delivered to the trig function is the angle we want plus an error angle proportional to the bits left behind in the accumulator. Substituting the approximate angle in the trig function and recognizing that the error angle is small, on the order of $2\pi\ 2^{-10}$, we can use the small angle approximation to extract the phase error term from the trig function as shown in (2).

$$\hat{\theta}(n) = \theta(n) + \theta_{Error}(n) \qquad (1)$$

$$\begin{aligned} e^{j\hat{\theta}(n)} &= e^{j[\theta(n)+\theta_{Error}(n)]} \\ &= e^{j\theta(n)}\, e^{j\theta_{Error}(n)} \\ &\cong e^{j\theta(n)}[1 + j\,\theta_{Error}(n)] \\ &= e^{j\theta(n)} + j\,\theta_{Error}(n)\,e^{j\theta(n)} \end{aligned} \qquad (2)$$

The results seen here is that, even with the phase angle errors, the desired carrier is present in the output which contains a second term seen to be the phase angle time series phase modulated to the carrier center frequency. It is this second term that is responsible for the spurs in the signal spectrum. Of course we can reduce the spur levels by reducing the amplitude of the phase error terms. This can be accomplished by using a wider bit field to represent the approximate phase angles.

An alternate approach is to recognize that the phase angle error is not random but, for this example, is $-2\pi/2^{48}$ times the bit field left behind by the quantization process. We can extract the error term by scaling the difference between the input and the output of the quantizer and use this term to obtain an improved estimate of the desired trig function values from the trig values formed with the quantized value of the angle. This relationship is seen in (3).

$$\theta_{Error}(n) = \theta(n) - \hat{\theta}(n) \qquad (3)$$

The feed forward correction applied to the output of the trig function is seen in (4). In a sense, this is the cosine and sine of the sum of two angles where we have replaced the cosine and sines of the small angle θ_{Error} by 1 and by and θ_{Error} respectively. A block diagram of the feed forward processing is shown in figure 4.

$$\begin{aligned} e^{j\hat{\theta}(n)} &= e^{j\theta(n)}\, e^{j\theta_{Error}(n)} \\ e^{j\theta(n)} &= e^{j\hat{\theta}(n)} e^{-j\theta_{Error}(n)} \\ &\cong e^{j\theta(n)} - j\,\theta_{Error}(n)\,e^{j\theta(n)} \\ &= [\cos(\hat{\theta}(n)) + \theta_{Error}(n)\sin(\hat{\theta}(n))] \\ &\quad + j\,[\sin(\hat{\theta}(n)) - \theta_{Error}(n)\cos(\hat{\theta}(n))] \end{aligned} \qquad (4)$$

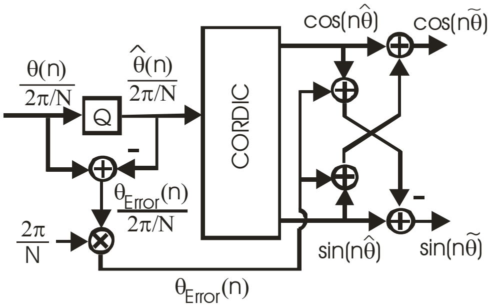

Figure 4. Block Diagram Feed Forward Angle Correction

The effect of the feed forward angle correction on the spectrum of the DDS output is quite dramatic. Figure 5, subplot (2,1,1) shows the spectrum formed with a 10 bit angle resolution corrected by the feed forward process of (4). Note the change in the y-axis scaling of figure 5 and figure 2, of -150 dB and -100 dB respectively. Note that the -60 dB spur level of figure 2 has been suppressed by the angle feed forward to -110 dB. We would have expected -

126 dB because we have removed the linear term of the phase Taylor series of size θ_{Error} leaving the quadratic term of the Taylor series of size $0.5{\cdot}\theta^2_{Error}$. There must be another error source for which we have not accounted. There is, it is the amplitude modulation imposed by the phase correction term (1 - j θ_{Error}).

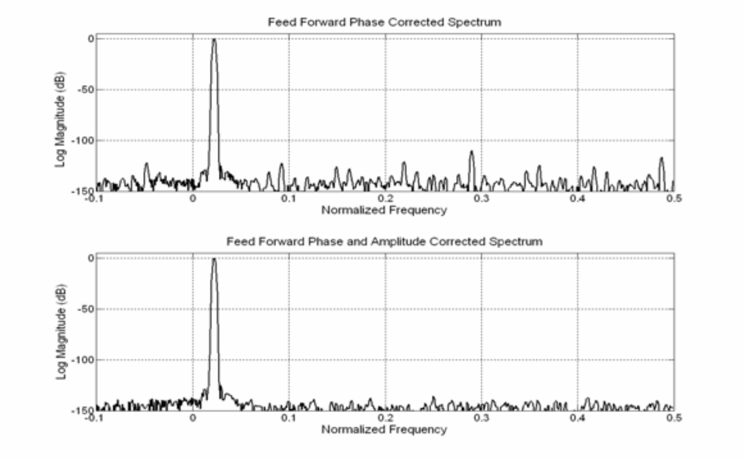

Figure 5. Spectra of DDS Output with 10-bit Angle Precision, with Phase Error Correction, and with Phase and Amplitude Error Correction

The actual rotation angle θ_{Rotate} imposed by the feed forward correction term (1 - j θ_{Error}) is described exactly by (5). This is precisely the angle relationship embedded in the CORDIC algorithm for values of $\tan(\theta_k) = 2^{-k}$. Each rotation in the CORDIC requires an amplitude correction equal to $\cos(\theta_k)$ which is applied at the end of the rotation sequence by a single product of the known correction terms. What is missing after the final phase error correction is the corresponding cosine amplitude correction.

$$\tan(\theta_{Rotate}) = \theta_{Error} \qquad (5)$$

To apply the amplitude correction we have to multiply the rotated I-Q pair by $\cos(\theta_{Rotate})$. When we corrected the amplitude in the CORDIC rotations we knew the values of the cosine and pre-computed the product of the cosine values. Since we don't know the precise correction angle beforehand we can't pre-compute its amplitude correction and we have to form an approximation based on the relationships shown in (6). Here we use the small argument approximation for the SQRT(1+e) and once again for the 1/(1+e/2). The correction term shown in (6) is applied as a scale factor to the outputs of the phase corrected terms as shown in figure 6. Note this term matches the first two terms of the cosine Taylor Series.

$$\cos(\theta_{Rotate}) = \frac{1}{\sqrt{1+\theta^2_{Error}}} \cong \frac{1}{1+\dfrac{\theta^2_{Error}}{2}} \cong 1 - \frac{\theta^2_{Error}}{2} \qquad (6)$$

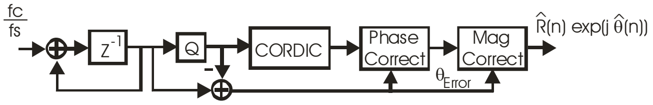

Figure 6. Signal Flow of Gain and Phase Corrected DDS

Figure 5, subplot(2,1,2), shows the spectrum obtained from a 10-bit precision angle CORDIC followed by the feed forward phase correction and again followed by the amplitude correction. The maximum spur level of the original 10-bit precise angle was -60 dB. When phase corrected, the spur dropped to -110 dB, and when amplitude corrected the spur fell below the noise floor with an observed maximum level of -132 dB. The arithmetic for this simulation used 20 bit multipliers with rounding for an expected numerical noise floor of -120 dB which when we include the processing gain of the 1024 point Kaiser-Bessel windowed FFT processing gain of approximately 25 dB becomes -145 dB. Without the benefit of ensemble averaging, the noise floor appears to be in the right neighborhood.

Figure 7 presents an interesting verification that the residual spur level in the DDS output after phase correction is the amplitude modulation. The three subplots of figure 6 are spectra of the DDS envelopes of the DDS, the phase corrected DDS, and the phase and amplitude corrected DDS. The envelopes have nominal amplitude of 1.0 which was treated as a bias and subtracted to enable detailed examination of the deviation from the nominal value. Note that the phase error correction increased the amplitude modulation spectral peak from -140 dB to -110 dB and that the amplitude error correction returned the level to -140 dB. The residual spectral noise floor is the amplitude noise due to finite precision of the trig table.

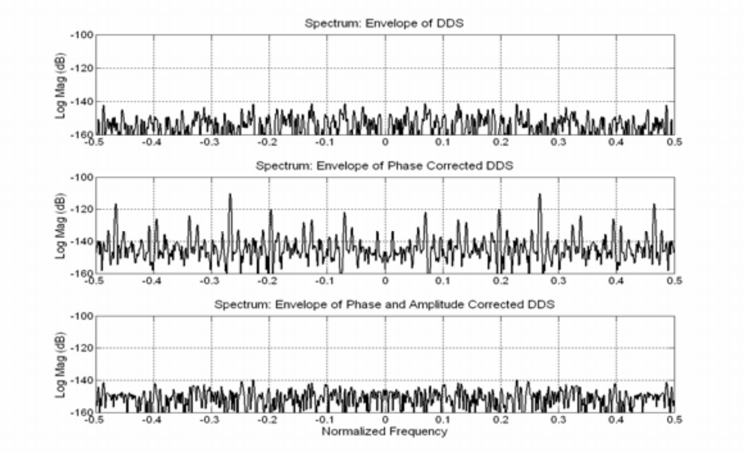

Figure 7. Spectra of DDS, Phase Corrected DDS, and Phase and Amplitude Corrected DDS Envelopes

3. EMBEDDING CORDIC PHASE AND AMPLITUDE CORRECTIONS IN RECUSIVE OSCILLATOR

The block diagram shown in figure 8 is a single pole feedback filter with a pole located on the unit circle at digital frequency θ radians/sample. A single iteration of this filter produces the same result as a 2x2 rotation matrix. The block diagram on the left of figure 9 illustrates the rotation as the formation of an output 2-tuple [x(n), y(n)] from the input 2-tuple [x(n-1), y(n-1)] in an architecture known as the normal filter [4, 5]. This rotation is shown explicitly in (7). When the cosine terms are factored from (7), as in (8), we obtain an alternate form of rotation, a tangent rotation, the core of the CORDIC algorithm shown as a filter on the right side of figure 9.

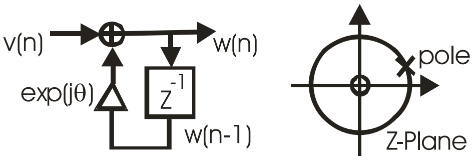

Figure 8. Single Pole Filer with Pole on Unit Circle

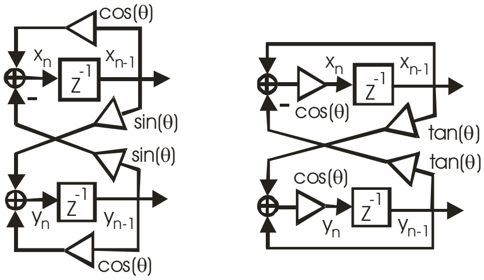

Figure 9. Normal and Tan Rotate Form of Single Pole Filter

$$\begin{aligned} x(n) &= x(n-1)\cdot\cos(\theta) - y(n-1)\cdot\sin(\theta) \\ y(n) &= y(n-1)\cdot\cos(\theta) + x(n-1)\cdot\sin(\theta) \end{aligned} \tag{7}$$

$$\begin{aligned} x(n) &= \cos(\theta)[x(n-1) - y(n-1)\cdot\tan(\theta)] \\ y(n) &= \cos(\theta)[y(n-1) + x(n-1)\cdot\tan(\theta)] \end{aligned} \tag{8}$$

The attraction of the normal filter structure is that the root locations reside on a Cartesian grid independently controlled by the filter coefficients. The real part of the root is equal to the feedback coefficient, cos(θ), around the filter register and the imaginary part equal to the cross couple coefficient, sin(θ), connecting the registers. This root distribution is illustrated in figure 10 which shows all possible root locations for coefficients implemented with 6-bit words.

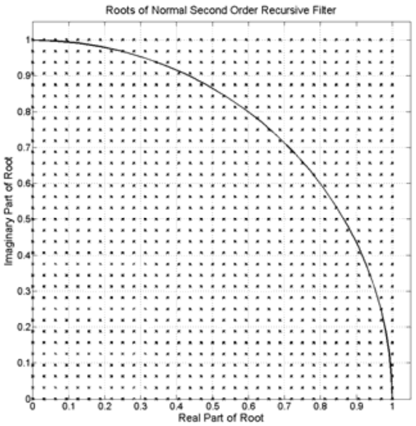

Figure 10. Root Distribution for 6-bit Quantized Coefficients of Normal Filter Architecture

We might be tempted to use one of the two forms of figure 9 as a complex sinusoid signal generator. Because the sine and cosine or the tangent and cosine in the two filters of figure 9 are transcendental numbers, and the arithmetic implementing the filter must be finite precision, the pole shown in figure 8 can not be precisely on the unit circle. Thus the pole is inside or outside and the response of either filter to an initial condition is an exponentially decaying or growing sinusoid. Look carefully at the root locations in the vicinity of the unit circle in figure 10. To use the filter as a complex sinusoid signal generator we would have to incorporate an AGC loop to stabilize its amplitude. The left side of figure 11 shows a redrawn version of the tan-rotate filter that incorporates an AGC mechanism to stabilize the filter amplitude. We note here that the cos(θ) multiply following the tan-rotate and the AGC scale factor "g" are both doing the same thing, scaling the ordered pair to obtain unity gain in the rotation. We want to keep the ordered pair on the unit circle! We elect to fold the cosine scale factor into the AGC scale factor, the standard approach in the CORDIC algorithm, and obtain the tan-rotate filter shown in the right side of figure 11.

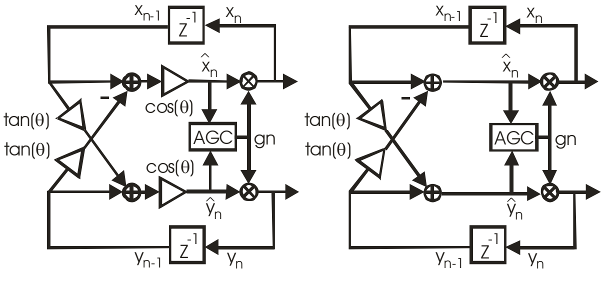

Figure 11. Tan-Rotate Filter with AGC, and Tan-Rotate Filter with Cosine Scale Embedded in AGC

We now replace the tan(θ) term in the tan-rotate block diagram with the CORDIC rotate and include a state machine to cycle the binary shifts and adds through their successive steps. This structure is shown in figure 12. The rotation process works in the following manner. The negative of the desired rotation angle is inserted in the servo accumulator. The CORDIC rotation engine performs (say) 10 iterations of binary shift and add of the ordered pairs [x(n-1),y(n-1)] while trying to zero the content of the servo accumulator by adding or subtracting the angles atan(2^{-k}) stored in the atan table. The AGC "g" is set to 1 for the first 9 iterations and at the 10th iteration is set to 1/1.646759, the product of the cosine scale factors is applied once at the end of the rotation cycle rather than once per rotation. There is assuredly a non-zero residual angle, θ_{Rem}, remaining in the servo accumulator. We perform one addition rotation by replacing the term 2^{-k} in the butterfly by the angle θ_{Rem}. This is the angle correction described in (4). We now have to perform the amplitude correction which because of the unknown arithmetic error terms in the recursion is not $1-\theta^2_{Rem}/2$ as it was 6. We must extract the correction term from the data sample.

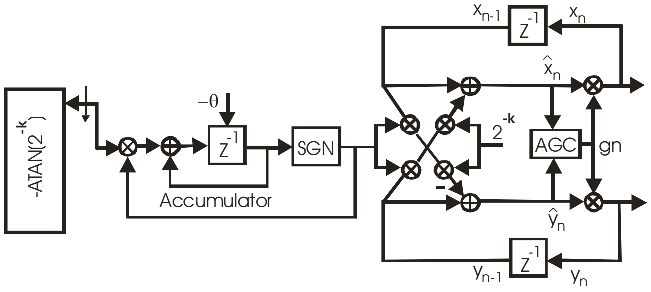

Figure 12. Tan-Rotate Filter with CORDIC Rotate and AGC Level Control

We assume that the rotation process resulted in an unknown amplitude increase ε relative to 1 which we indicate in (9). We apply the gain "g" to the outputs of the final rotation to obtain the results shown in (10). Solving for the gain, we determine the relationship shown in (11). It appears that we have a problem, we really don't know the error ε. But in fact we do! We can solve for it from (9) and substitute in (11) to obtain (12).

$$\hat{x}^2(n)+\hat{y}^2(n)=\{1+\varepsilon\} \tag{9}$$

$$[\hat{x}^2(n)+\hat{y}^2(n)]\cdot g^2=\{1+\varepsilon\}\cdot g^2=1 \tag{10}$$

$$\begin{aligned} g^2 &= \frac{1}{\{1+\varepsilon\}}, \\ g &= \frac{1}{\sqrt{1+\varepsilon}} \cong \frac{1}{1+\dfrac{\varepsilon}{2}} \cong 1-\frac{\varepsilon}{2} \end{aligned} \tag{11}$$

$$\begin{aligned} \varepsilon &= [\hat{x}^2(n)+\hat{y}^2(n)]-1 \\ g &= 1-\frac{\varepsilon}{2} = 1-\frac{[\hat{x}^2(n)+\hat{y}^2(n)]-1}{2} \\ &= \frac{3-[\hat{x}^2(n)+\hat{y}^2(n)]}{2} \end{aligned} \tag{12}$$

The AGC gain term "g" of (12) applied to the output of the tan rotate and angle correction rotate operates in the direction to correct the amplitude error caused by the phase correction as well amplitude increase or decrease due to the pole position error relative to the unit circle. Figure 13, subplot(2,1,1) shows the spectrum of a complex sinusoid formed with the recursive CORDIC and stabilized with the AGC mechanism described in (12). Subplot(2,1,2) shows the AGC gain less its nominal unity value. In this example the CORDIR ran 10 iterations, and the arithmetic used 20 bit multipliers.

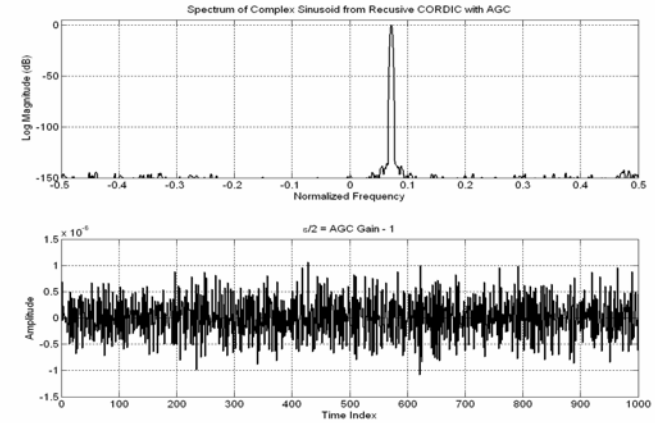

Figure 13. Spectrum: Complex Sinusoid from Recursive CORDIC with AGC and Gain Correction Term Time Series

An interesting aspect of the recursive CORDIC is that for a fixed frequency sinusoid, the servo accumulator is initialized with the same angle value for each successive time sample. Thus the sequence of add-subtract iterations in the CORDIC is identical for each computed trig sample. The memory of the recursive CORDIC resides in the filter states rather than in the traditional phase accumulator which forms and presents a sequence of phase angles modulo 2π to the CORDIC's servo accumulator. Thus the phase error sequence is a constant for the recursive CORDIC, it is always the same angle error residing in the servo accumulator. Consequently there is no line structure in the spectrum of recursive CORDIC and the phase error correction is not applied to suppress phase error artifacts but rather to complete the phase rotation left incomplete due to the residual phase term in the servo accumulator. This is a very different DDS! A practical note related to recursive filters. There are quantizers between the summing junction feeding the CORDIC registers and the registers. The truncation circulates in the registers and contributes a DC term, hence a spectral line to the complex sinusoid. This DC term can be (should be) suppressed by using a sigma delta feedback loop to feedback the truncated segments of the sums. A final comment about the data dependent AGC used in the recursive CORIC. This process can also be used in the non recursive CORDIC following the feed forward phase correction as a replacement option for the deterministic phase error related correction shown in (6).

4. CONCLUSIONS

We have reviewed the structure of traditional DDS quadrature sinusoidal signal generators. This structure contains a phase accumulator, a quantizer, and an angle-to-amplitude conversion process which is either a look-up table or a CORDIC rotator. We also reviewed the relationship between the width of the bit field taken from the phase accumulator by the quantizer and the spurious levels seen in the spectra of the carrier. We recognized that the spurs were related to the phase error caused by leaving bits behind in the phase accumulator. Knowing the error we reviewed the process that feeds the error forward to suppress the spurs. A contribution to the art made in this paper is our recognition that the phase correction induced an amplitude modulation and that if the amplitude modulation is similarly suppressed a significant reduction in spurs can be had relative to the already significant reduction due to the phase correction. We developed and presented the process required to compensate for the amplitude modulation.

Recognizing that the amplitude control was akin to an AGC we embedded the CORDIC, the phase correction, and the amplitude correction in a first order recursive filter with a pole located close to, but not precisely on the unit circle. The performance of a DDS with the recursive structure is quite remarkable and we suggest that you, the reader, might want to take a careful look at its structure.

5. REFERENCES

[1] J. Vallis, T. Sansaloni, A. Perez-Pascual, V. Torres, and V. Almenar, “The Use of CORDIC in Software Defined Radios: A Tutorial”, IEEE Communications Magazine, Vol. 44, No. 9, pp. 46-50, Sept. 2006.

[2] Chis Dick, fred harris, and Michael Rice, “Synchronization in Software Defined Radios – Carrier and Timing Recovery Using FPGAs”, IEEE Symposium On Field-Programmable Custom Computing Machines, Napa Valley CA, April 16-19, 2000

[3] fred harris and Bill McKnight, “Error Feedback Loop Linearizes Direct Digital Synthesizers”, 29-th Asilomar Conference on Signals, Systems, and Computers, pp.98-102, Pacific Grove, CA, 30-Oct. to 2-Nov. 1995.

[4] Sanji .K. Mitra, “Digital Signal Processing: A Computer-Based Approach”, 2006, Ch 8.11, McGraw Hill, NY, NY.

[5] fred harris, “A Novel Approach to the Design of Optimal Second Order Digital Filters”, SOUTHCON-82; Orlando, FL, March 1982.